Available online at www.sciencedirect.com
SCIENCE DIRECT®
International Journal of Mass Spectrometry 244 (2005) 164–170
International Journal of Mass Spectrometry
www.elsevier.com/locate/ijms

Surface collisions of formic acid cations $HCOOH^+$ and $DCOOD^+$ with a hydrocarbon-covered stainless steel surface

Thawatchai Tepnual [a], Linda Feketeová [a], Verena Grill [a,*], Paul Scheier [a], Zdenek Herman [a,b], Tilmann D. Märk [a,c]

[a] *Institut für Ionenphysik, Leopold-Franzens Universität, Technikerstr. 25, A-6020 Innsbruck, Austria*
[b] *V. Čermák Laboratory, J. Heyrovský Institute of Physical Chemistry, Academy of Sciences of the Czech Republic, Dolejškova 3, CZ-182 23 Prague 8, Czech Republic*
[c] *Department of Experimental Physics, Comenius University, Mlynska Dolina, 842 15 Bratislava 4, Slovak Republic*

Received 5 April 2005; received in revised form 21 June 2005; accepted 22 June 2005

Abstract

Interaction of the formic acid cation $HCOOH^+$ with a stainless steel surface covered with hydrocarbons has been studied as a function of the collision energy from a few eV up to 40 eV. Mass spectra of the product ions showed ions produced by surface-induced dissociation of the projectile and formation of $HCO_2H_2^+$ in interaction with the surface material. The fragmentation of the projectile led to product ions $HCOO^+$ and CHO^+. The product ion $HCO_2H_2^+$ fragmented to give only CHO^+, indicating that its structure was $HC(OH)_2^+$ as suggested earlier by others. The results were confirmed by studies using the deuterated formic acid cation $DCOOD^+$.

Keywords: Formic acid; Surface-induced dissociation; Surface-induced reaction

1. Introduction

Interaction of low energy (1–100 eV) ions with solid surfaces has received increasing attention during the past years [1,2]. In particular, surface collisions of polyatomic ions show a variety of processes and render them a quite interesting research project. The processes occurring upon surface collisions in the hyperthermal energy range include: (i) charge exchange and neutralization of projectile cations or partial or full neutralization of doubly charged ions; (ii) elastic scattering; (iii) inelastic scattering followed by dissociation of the projectile ions, (surface-induced dissociation, SID) [3,4]; (iv) chemical reactions of projectile ions with the surface material; and (v) chemical sputtering of adsorbates from the surface [5,6]. Studies of collision energy resolved mass spectra (CERMS) of product ions from surface collisions can provide useful information on the nature of both the polyatomic ions and of the surface [3,7,8].One of the important characteristics of surface collisions which renders them superior to gas phase collisions (in a similar energy range) is the fact that the internal energy distribution transferred during the collision is narrower and that the maximum of the transferred energy scales with the collision energy [9]. Therefore, surface collisions may be used in surface activation-and-fragmentation even of large molecules and biomolecules making it a useful tool for structure elucidation and characterization of the projectile ion [10].

Formic acid (HCOOH) is the simplest carboxylic acid in which the carboxyl group –COOH is bound to R = H. The carboxyl group is common to several complex (and often biologically relevant) molecules and formic acid thus may represent a suitable model compound for understanding the behavior of more complicated molecules. Apart from being an important industrial product, HCOOH is also well known to play a role in human metabolism, and in atmospheric as well as interstellar chemistry [11]. It can be found in a variety of plants, fruits, mammalian tissues, and insect venoms

* Corresponding author. Tel.: +43 512 507 6250; fax: +43 512 507 2932.
E-mail address: verena.grill@uibk.ac.at (V. Grill).

1387-3806/$ – see front matter © 2005 Elsevier B.V. All rights reserved.
doi:10.1016/j.ijms.2005.06.008

and it is also used industrially as a preservative and antibacterial in livestock feed [12]. Formic acid is also a polluter of air and water and has been identified as a toxic intermediate (formate) in methanol poisoning [13]. Because formic acid is one of the possible building blocks of biomolecules [14], the study of this molecule is of interest for both exobiology and astrophysics, in particular regarding the question of molecule formation. Although the formic acid ion $HCOOH^+$ or other stable isomers of the general formula $CH_2O_2^+$ [15,16] have not been observed directly in the interstellar medium, decomposition products such as the formyl radical ion HCO^+, which plays an important role in molecule formation in interstellar clouds [17], and protonated carbon dioxide, $HOCO^+$, have been observed [18].

Several experimental studies have been performed with formic acid. Schwell et al. [19] studied the VUV photofragmentation of formic acid over the 6–23 eV energy range and reported dissociative photoionization of $HCOOH + h\nu \rightarrow COOH^+ + H$ and $HCOOH + h\nu \rightarrow HCO^+ + OH$ with an energy threshold of 12.22 and 12.79 eV, respectively. In their photoionization study, Berkowitz et al. [20] deduced the heat of formation of the carboxyl cation $COOH^+$ by measuring its dissociative ionization threshold from HCOOH. In an adjacent paper [21], the same authors report on the stability of the different structures of the carboxyl cation, i.e., $COOH^+$ versus $HCOO^+$. The authors found evidence for a higher stability of the $COOH^+$; however, Burgers et al. [22] reported that $HCOO^+$ was sufficiently stable to survive at least 10 μs before rearranging to $COOH^+$; therefore, at short times, both structures may be present. In an electron attachment study performed recently in the Innsbruck lab [23], low energy electrons have been used in a high-resolution experiment to produce three anionic fragments $HCOO^-$, OH^- and O^-.

In addition to these experimental studies, HCOOH has attracted attention of several theoretical groups. The structure and energetics of $HCOO^+$ and $COOH^+$ produced from formic acid have been investigated by Yu et al. [24] using the multiconfigurational self-consistent field theory. Uggerud et al. [16] and Ruttnik and Burgers [25] performed ab initio calculations (using unrestricted and restricted Hartee–Fock procedures) to calculate the potential energy surface of the $CH_2O_2^+$ system.

In this paper, we describe the results of surface collisions of formic acid cations $HCOOH^+$ formed after electron impact ionization of formic acid. The projectile ion collided with a stainless steel surface (covered at room temperature by hydrocarbons) and product ion mass spectra were recorded as a function of the collision energy (from a few eV to 40 eV).

2. Experimental

Experiments were carried out with the tandem mass spectrometer apparatus BESTOF described in detail in our earlier papers [26,27]. It consists of a double-focusing two-sector field mass spectrometer (reversed geometry) combined with a linear time-of flight mass spectrometer (see Fig. 1). In short, the formic acid vapor was directly introduced into a Nier-type ion source (pressure 1.5×10^{-5} Torr) and ionized by electron impact of a 99 eV electron beam (nominal energy in the experiments; unfortunately, variation of electron energy close to the ionization energy of formic acid – to influence the internal energy content of the projectile ion – was not possible in these experiments). The ions produced were extracted from the source region, focused and accelerated to about 3 keV for mass analysis by the double-focusing two-sector field mass spectrometer. After passing the exit slit of the mass spec-

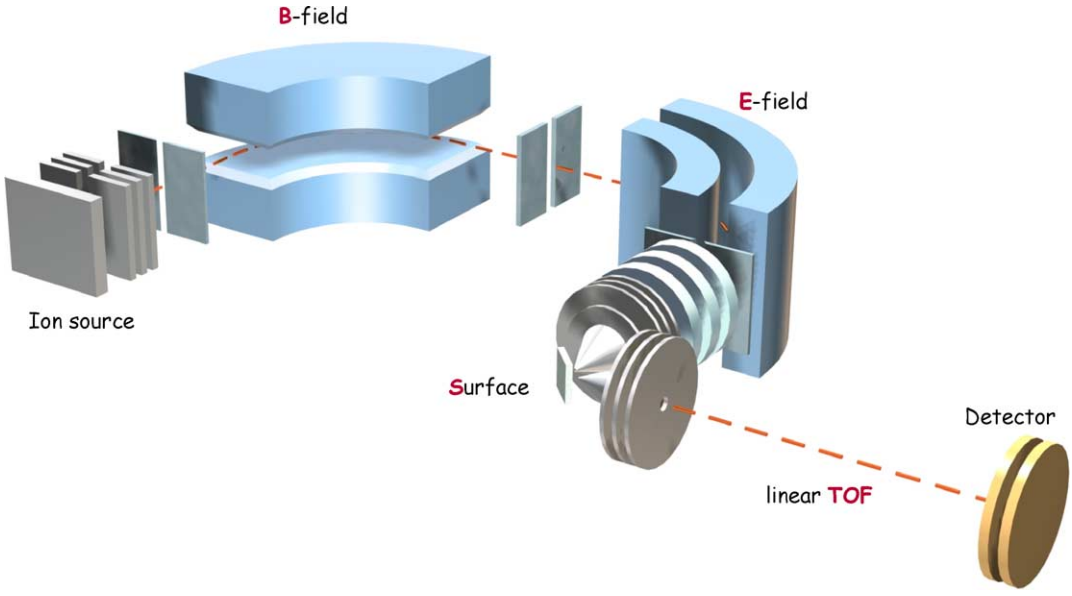

Fig. 1. Schematic view of the experimental set-up consisting of the Nier-type ion source, a two-sector field mass spectrometer for projectile ion preparation, a target surface chamber, and a time-of-flight mass spectrometer for detection of product ions.

trometer, the ions were refocused by an Einzel lens to the deceleration optics placed in front of the stainless steel surface. Field penetration effects were minimized by shielding the surface with conical-shaped lenses. The collision energy of the ions impacting on the surface is defined by the potential difference between the ion source and the surface and can be varied from about 0 to about 2 keV. The incident angle of the primary ions on the surface was kept at 45° and the scattering angle was fixed at 91° with respect to the direction of incident ion beam. The energy spread of the projectile beam was about 200 meV (full-width-at half-maximum). It was determined by applying to the target a retarding potential and measuring the (reflected) total ion signal as a function of the target potential. Product ions formed at the surface leave the shielded chamber through a 1 mm diameter orifice and are then subject to the extraction and acceleration field of the second mass spectrometer (a linear time-of-flight mass spectrometer with a flight tube of about 80 cm length). The mass selected ions are detected by a double-stage multi-channel plate, which is connected to a multi-channel analyzer (time resolution of 5 ns per channel) and a laboratory computer. The background gas pressure in the target region was about 2×10^{-9} Torr. Even at this pressure, however, the stainless steel surface (at room temperature) was covered by hydrocarbons originating presumably from cracked pump oil. Hydrocarbon-covered metal or carbon surfaces have been used in many ion-surface collision studies [3,4,26–32]. It is a very stable and reproducible surface; heating to above 600° C essentially removes [33] the hydrocarbon layer and cooling back to room temperature re-establishes it within a few hours, with the same properties (within the experimental error). The properties of the hydrocarbon-covered surface (energy partitioning, fragmentation of projectiles, chemical reactions) were shown [31] to be very similar to those of a surface covered with a hydrocarbon C_{12} self-assembled monolayer.

3. Results and discussion

The most abundant ion in the electron impact mass spectrum of the formic acid vapor (HCOOH) at 99 eV was the fragment ion at *m*/*z* 29 (CHO^+). The abundance of the parent ion at *m*/*z* 46 ($HCOOH^+$) and the fragment ion at *m*/*z* 45 ($HCOO^+$) was about 75 and 92.5% of the most abundant ion, respectively. Other abundant ions were the fragment ion at *m*/*z* 44 (30%), corresponding to $CO_2{}^+$, at *m*/*z* 28 (about 30%), corresponding to CO^+, and the fragment ion at *m*/*z* 18 (H_2O^+). All other ions present in the mass spectrum had an abundance of less than 5%. The formulas above indicate only the elemental ion composition and not the actual structure of the ions (e.g., $HCOO^+$ versus $COOH^+$).

The product ion mass spectra upon surface impact of $HCOOH^+$ can be seen in Fig. 2 for several selected collision energies up to 30 eV. A clearly distinguishable product fragment ion was at *m*/*z* 29 (CHO^+), appearing at collision energies higher than 7 eV. The intensity of the fragment ion

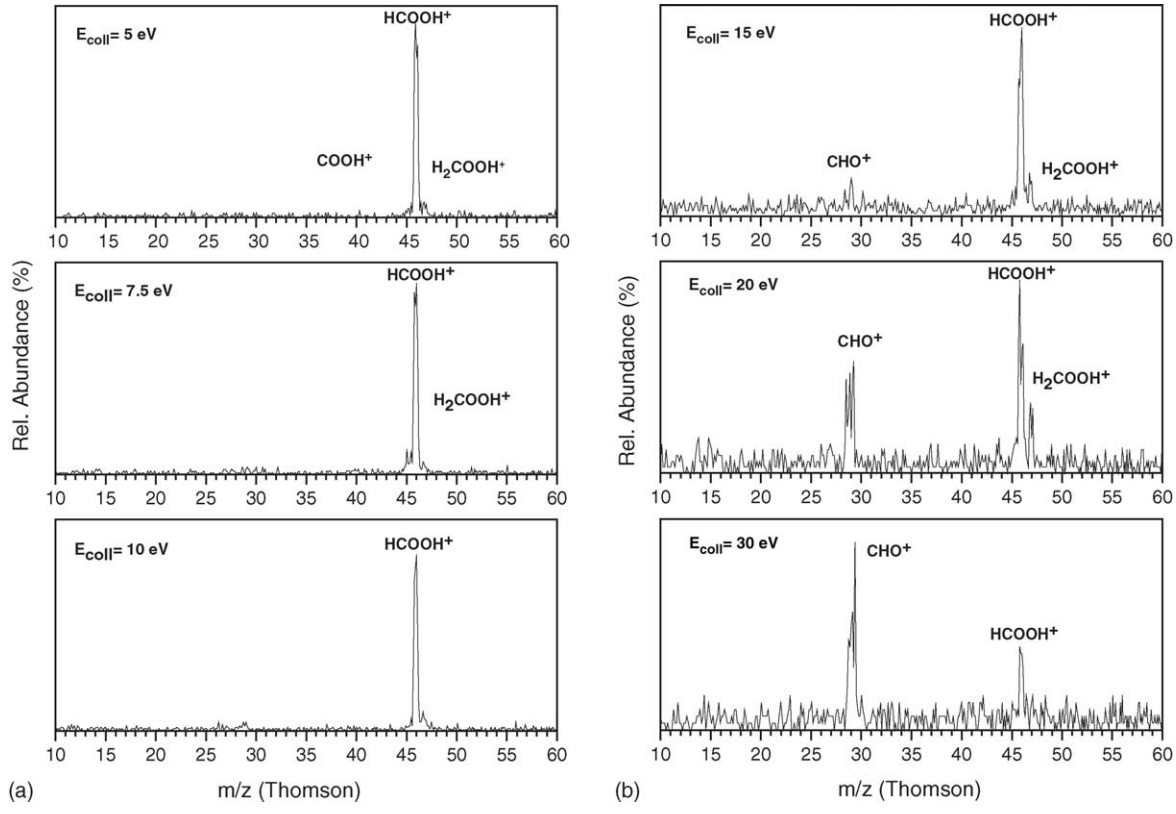

Fig. 2. Mass spectra of product ions from surface collisions of the $HCOOH^+$ projectile ion at collision energies of 5, 7.5, 10, 15, 20 and 30 eV.

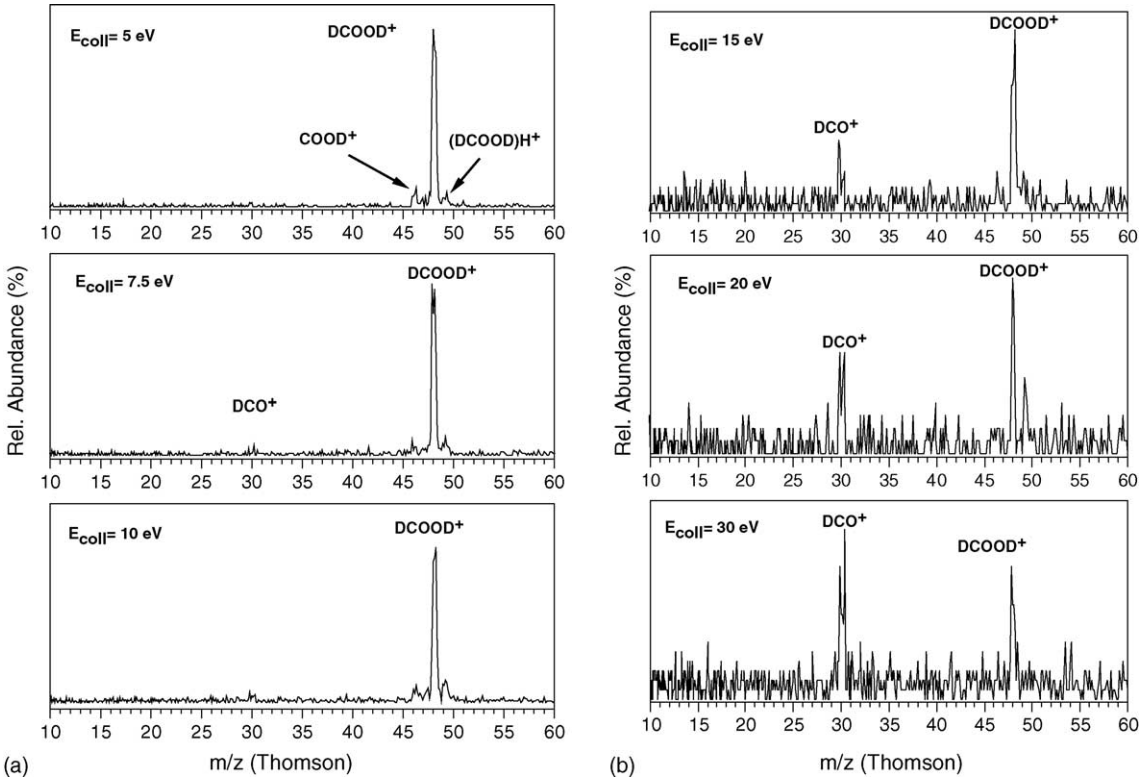

Fig. 3. Mass spectra of product ions from surface collisions of the $DCOOD^+$ projectile ion at collision energies of 5, 7.5, 10, 15, 20 and 30 eV.

at *m*/*z* 45, corresponding to a loss of an H atom from the projectile ion, was difficult to estimate precisely due to the broadening of the TOF peak of the non-dissociated projectile molecular ion. On the other hand, the $HCO_2H_2^+$ ion at *m*/*z* 47, formed by a H-atom pick-up from the surface material, could be identified at incident energies of 5 eV and higher, as the molecular peak slope on the high-mass side was much steeper. Fig. 3 summarizes data on surface collisions of the deuterated formic acid molecular ion, $DCOOD^+$, with the surface over the same collision energy range as for $HCOOH^+$. Here, the fragment ion $DCOO^+$ could be clearly distinguished at *m*/*z* 46 with an onset at the incident energy of about 7 eV. This fragment ion begins to decrease above about 15 eV and it disappears completely at 30 eV. In addition a small intensity (comparable or smaller than the intensity at *m*/*z* 46) could be observed at *m*/*z* 47 in the spectra at collision energies 5, 7.5, 10 and 15 eV. This H-atom pick-up reaction from the surface hydrocarbons and formation of $DCOODH^+$ can be observed in the energy range from 5 to about 20 eV, similar as for the $HCOOH^+$ projectile ion.

For a better understanding of the surface-induced fragmentation of the formic acid cation, the collision energy resolved mass spectra (CERMS) curves for both the hydrogenated and the deuterated formic acid were derived from the data (Fig. 4a and b). It can be seen that the onsets and the relative abundance of the respective fragment ions are very similar for both projectiles, $HCOOH^+$ and $DCOOD^+$.

As mentioned earlier, fragmentation of the molecular ion of the formic acid, energetics of the species and processes involved was subjected to several studies. The break-down pattern of the molecular ion was obtained by Niwa et al. from results of a photoelectron-photoion coincidence spectroscopy study [34]. In their break-down diagram for the formic acid molecular ion, the parent ion $HCOOH^+$ persists as the only ion up to the internal energy of 0.7 eV and then it quickly vanishes. It is replaced by the ion $HCOO^+$ (*m*/*z* 45) that dominates the break-down graph in the energy range from 0.7 to 1.3 eV (relative abundance 100%) and then it decreases to about 30%. At 1.3 eV, the abundance of fragment ions of *m*/*z* 29 (CHO^+) and 18 (H_2O^+) starts to increase sharply over an energy range 1.3–1.6 eV to about 40% each. Over the range of internal energies 1.6–3.2 eV, the abundance of *m*/*z* 18 quickly decreases to about 5%, while the abundance of *m*/*z* 29 continues to increase to about 65%. Between 3 and 6 eV, the abundance of *m*/*z* 45, 29 and 18 remains basically the same with oscillations above 4 eV, ascribed to isolated excited electronic states of the molecular ion. The ionization energy of formic acid is taken in this paper as IE = 11.33 eV, in agreement with the data of [34] and tabulated data [35]. Dissociative photoionization of $HCOOH^+$ to $HCOO^+$ was subjected to other detailed studies and was shown to involve both direct bond cleavage and a rearrangement process of $HCOOH^+$ to $C(OH)_2^+$ (with an activation barrier of at least 90 kJ/mol) [20,21].

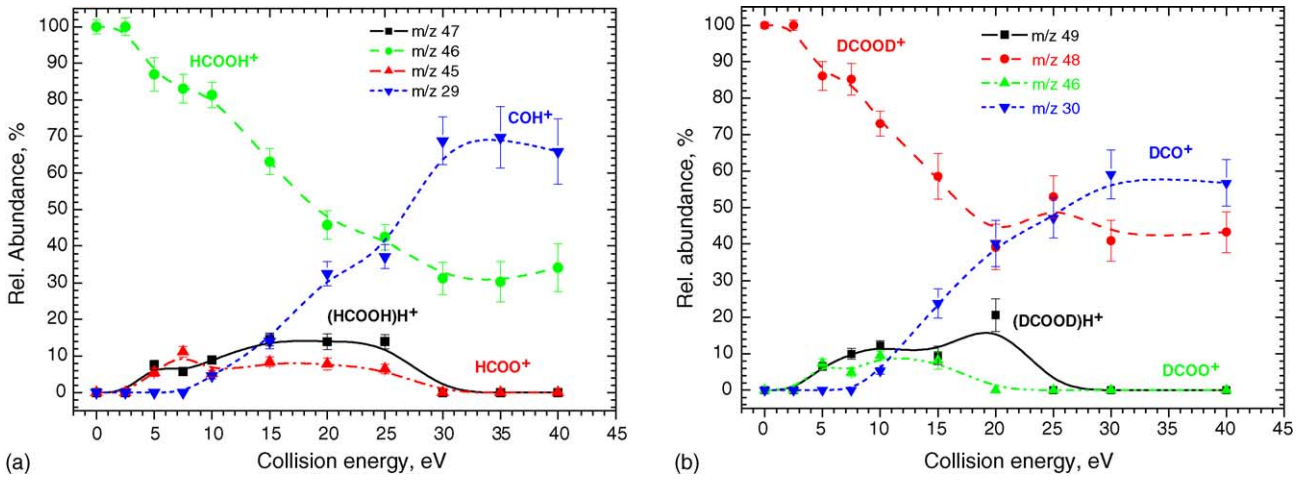

Fig. 4. Collision energy resolved mass spectra (CERMS curves) from surface collisions of the $HCOOH^+$ (a) and $DCOOD^+$ (b) projectile ion. The ordinate is given as percentage of abundance of all product ions detected.

The CERMS curves reflect information on the energetics of the processes involved. In the following, some CERMS features are used in an approximate comparison with features in the break-down pattern. For this, one has firstly to take into account that the projectile ions in the present study were formed by electron impact ionization in the low-pressure Nier-type source. This mode of ionization produces the ions with a distribution of internal energies and this initial internal energy of the projectile was shown [30,31] to be fully effective in the surface collision-induced fragmentation processes. Using the break-down pattern [34] and the photoelectron spectrum of formic acid [36], the initial internal energy of the formic acid projectile ion can be estimated (for more details see [30,31]) to range from 0 to 0.7 eV with a maximum at about 0.2 eV. Second, internal energy acquired by the projectile in surface excitation is well established for this type of surfaces (metal surface covered with hydrocarbons) to be 6% of the incident translational energy [30–32] with a full-width-at-half-maximum (FWHM) of about 2 eV and full width close to 3.5–4 eV. Thus, the collision range in this study (from close to 0 to 40 eV) covers the range of surface collision-induced internal excitation (0.06×40 eV maximum) of up to 2.4 eV. The broadening of the energy transferred in the surface collision to internal excitation (FWHM of 2 eV) moreover represents a very substantial part of this energy range.

With these informations, it is possible to analyse quantitatively (see also [30,31]) the onset of the formation of CHO^+ (between 7.5 and 10 eV) and the crossing between the CERMS curves of $HCOO^+$ and CHO^+ at 11 eV(see Fig. 4 a and b). Taking the average of energy transferred to internal energy 0.06×7.5 eV = 0.45 eV and adding the initial energy of the projectile ion (0.7 eV), we arrive at an energy threshold for CHO^+ formation of 1.2 eV which compares well with the value of 1.2 eV derived from the break-down curves [34]. Similarly, for the crossing between the CERMS curves of CHO^+ and $HCOO^+$, we obtain a value of $(0.06 \times 11 + 0.7)$ eV = 1.4 eV to be compared with the value of 1.6 eV from the break-down pattern [34] and the value of 1.4 eV derived in the work of Uggerud et al. [16].

The CERMS curves in Fig. 4a and b indicate a rather small contribution of the fragment ions of *m/z* 45 ($HCOO^+$) or *m/z* 46 ($DCOO^+$), though this ion dominates the break-down pattern over a substantial range of internal energies [34]. Also, the fragment ion H_2O^+ (D_2O^+) does not appear in measurable amounts among the fragmentation products in the break-down graph. On the other hand, the molecular ion stretches over the entire range of collision energies and even at 40 eV its relative abundance is close to 30%. This can be explained by a rather wide range of energies transferred into internal energy of the projectile upon surface interaction. As mentioned above, the expected width of the energy transferred (FWHM about 2 eV) translates into a substantial part of the collision energy range covered by the CERMS curves (with the collisional-to-internal energy transfer of 6%, 2 eV mean more than 30eV). Even though the maximum shifts with increasing collision energy, this energy width means that even at 40 eV, there is a certain probability of transferring into internal energy of the projectile less than 0.7 eV and this can lead to formation of non-dissociated projectile ions. The spread of transferred energy in surface collisions can then result in broadening and averaging over a substantial region of the break-down pattern and to different product ion abundance in the CERMS curves, even if the surface-induced fragmentation basically follows the unimolecular pattern.

In addition, the product ions formed in interaction of the projectile with the hydrocarbon-covered surface result from fragmentation of more than the projectile ion, namely of the projectile ion and of the $HCO_2H_2^+$ ion, formed in hydrogen atom transfer from the surface material to the projectile. This is quite plausible. First of all, formation of this ion was observed as a product of surface interaction of both $HCOOH^+$ ($HCO_2H_2^+$)and $DCOOD^+$ ($HCO_2D_2^+$) projectiles at *m/z* 47 and 49, respectively. The proton affinity of formic acid, 742kJ/mol [37], is comparable to those of methanol

(754 kJ/mol), ethanol (776 kJ/mol) and benzene (750 kJ/mol) and the molecular ions of these compounds are known to form protonated products in interaction with the hydrocarbon-covered surfaces [25,31,38]. The undissociated protonated product ion can be detected both in the spectra of $HCOOH^+$ (*m*/*z* 47) and $DCOOD^+$ (*m*/*z* 49). It can be expected to dissociate preferentially to form CHO^+ (CDO^+), as suggested by Sekiguchi et al. [39]. In their CID spectra of the protonated formic acid, these authors observed only the formation of HCO^+ (not of H_3O^+) and this led them to conclude that the protonated formic acid beam was composed almost exclusively of $HC(OH)_2{}^+$. The same holds for our results (no fragmentation to H_3O^+ observed) and thus their conclusion concerning the structure of the protonated moiety presumably holds also for our surface protonated formic acid projectile. However, the CERMS curves show that the decomposition of the surface-protonated formic acid is responsible for only a fraction of the product ions (up to about 20%) as indicated by the relative abundance of the ion $HCO_2H_2{}^+$ and an increase of its dissociation product CHO^+ (CDO^+) at higher collision energies.

The main decomposition channel appears to be fragmentation of the surface-excited formic acid ion, presumably its rearranged, more stable structure $HOCOH^+$ ($DOCOD^+$) as discussed by Uggerud et al. [16]. The time-of-flight of a formic acid cation from the ion source to the surface in the present experimental set-up is in the order of 15 μs which leaves enough time for the excited formic acid ion to rearrange. The non-observance of the product ions H_2O^+, $CO_2{}^+$ and CO^+ may be then connected with the high activation barrier (about 2 eV) needed in the rearrangement process necessary for their formation [16].

4. Conclusions

Collisions of the formic acid cations $HCOOH^+$ and $DCOOD^+$ with a stainless steel surface covered with hydrocarbons were studied over the collision energy range from a few eV up to 40 eV. The fragmentation of the projectile ions was found to result from dissociation of the surface-excited projectile and from dissociation of the protonated formic acid ion formed in the interaction of the projectile ion with hydrogen of the surface material. Dissociation processes of the projectile ion led to the formation of fragment ions $HCOO^+$ ($DCOO^+$) and CHO^+ (CDO^+). Dissociation of the ion $HCO_2H_2{}^+$ ($HCO_2D_2{}^+$) led to the formation of CHO^+ (CDO^+), no dissociation to H_3O^+ was observed. This suggests that the prevailing structure of the dissociating protonated formic acid was $HC(OH)_2{}^+$ as suggested earlier from other studies [39].

Acknowledgements

This work has been carried out within the Association EURATOM-ÖAW in cooperation with the Association EURATOM-IPP.CR. The content of the publication is the sole responsibility of its publishers and it does not necessarily represents the view of the EU Commission or its services. Work was also partly supported by the FWF, ÖAW and ÖNB, Wien, Austria, and the network program of the European Commission, Brussels. Partial support of this research by the Grand Agency of the Academy of Sciences of the Czech Republic (No. 4040405) is gratefully acknowledged.

References

[1] Y. Murata, in: C.Y. Ng, T. Baer, I. Powis (Eds.), Unimolecular and Bimolecular Reaction Dynamics, Wiley, New York, 1994.
[2] L. Hanely (Ed), Polyatomic Ion-Surface Interactions, Int. J. Mass Spectrom., 174, 1998.
[3] Md.A. Mabud, M.J. DeKrey, R.G. Cooks, Int. J. Mass Spectrom. Ion Processes 67 (1985) 285.
[4] W.R. Koppers, M.A. Gleeson, J. Lourenco, T.L. Weeding, J. Los, A.W. Kleyn, J. Chem. Phys. 110 (1999) 2588.
[5] R.G. Cooks, T. Ast, Md.A. Mabud, Int. J. Mass Spectrom. Ion Processes 100 (1990) 209.
[6] V. Grill, J. Shen, C. Evans, R.G. Cooks, Rev. Sci. Instrum. 11 (2003) 3149.
[7] R. Wörgötter, C. Mair, T. Fiegele, V. Grill, T.D. Märk, H. Schwarz, Int. J. Mass Spectrom. Ion Processes 164 (1997) 1.
[8] S.B. Wainhaus, H. Lim, D.G. Schultz, L. Hanley, J. Chem. Phys. 106 (1997) 10329.
[9] T. Ast, J. Serb. Chem. Soc. 66 (2001) 735.
[10] M.J. Hayward, Md.A. Mabud, R.G. Cooks, J. Am. Chem. Soc. 110 (1988) 1343.
[11] J.M. Girart, A. Temijan, L.E. Snyder, Astrophys. J. 576 (2002) 255.
[12] http://www.brainyencyclopedia.com/encyclopedia/f/fo/formic_acid.html.
[13] M. Thomson, NTP Technical Report on Toxicity Studies of Formic Acid, National Toxicology Program, Toxicity Report Series, Number 19, 1992.
[14] A. Brack (Ed.), The Molecular Origins of Life, Cambridge University press, Cambridge, UK, 1998.
[15] P.A. Burgers, A.A. Mommers, J.L. Holmes, J. Am. Chem. Soc. 105 (1983) 5976.
[16] E. Uggerud, W. Koch, H. Schwarz, Int. J. Mass Spectrum. Ion Processes 73 (1986) 187.
[17] E. Herbst, Chem. Soc. Rev. 30 (2001) 168.
[18] M.C. McCarthy, P. Thaddeus, Chem. Soc. Rev. 30 (2001) 177.
[19] M. Schwell, F. Dulieu, H.W. Jochims, J.-H. Fillion, J.-L. Lemaire, S. Baumgärtl, S. Leach, J. Phys. Chem. A 106 (2002) 10908.
[20] B. Ruscic, M. Schwarz, J. Berkowitz, J. Chem. Phys. 91 (1989) 6772.
[21] B. Ruscic, M. Schwarz, J. Berkowitz, J. Chem. Phys. 91 (1989) 6780.
[22] P.C. Burgers, J.L. Holmes, J.E. Szulejko, Int. J. Mass. Spectrom. Ion Processes 57 (1984) 159.
[23] A. Pelc, W. Sailer, P. Scheier, N.J. Mason, T.D. Märk, Eur. Phys. J. D20 (2002) 441.
[24] J.G. Yu, X.Y. Fu, R.Z. Liu, K. Yamashita, N. Koga, K. Morokuma, Chem. Phys. Lett. 125 (1986) 438.
[25] P.J.A. Ruttink, P.C. Burgers, Int. J. Mass Spectrom. Ion Processes 113 (1992) 23.
[26] C. Mair, T. Fiegele, F. Biasioli, J.H. Futrell, Z. Herman, T.D. Märk, Int. J. Mass. Spectrom. 188 (1999) L1.
[27] V. Grill, R. Wörgötter, J.H. Futrell, T.D. Märk, Z. Phys. D40 (1997) 111.

[28] A. Qayyum, T. Tepnual, C. Mair, S. Matt-Leubner, P. Scheier, Z. Herman, T.D. Märk, Chem. Phys. Lett. 376 (2003) 539.
[29] A. Qayyum, Z. Herman, T. Tepnual, C. Mair, S. Matt-Leubner, P. Scheier, T.D. Märk, J. Phys. Chem. A 108 (2004) 1.
[30] J. Kubišta, Z. Dolejšek, Z. Herman, Eur. Mass Spectrom. 4 (1998) 311.
[31] J. Žabka, Z. Dolejšek, Z. Herman, J. Phys. Chem. A 106 (2002) 10861.
[32] Z. Herman, Int. J. Mass Spectrom. 233 (2004) 361.
[33] J. Roithová, J. Žabka, Z. Dolejšek, Z. Herman, J. Phys. Chem. B 120 (2002) 8293.
[34] Y. Niwa, T. Nishimura, F. Isogai, T. Tsuchiya, Chem. Phys. Lett. 74 (1980).
[35] S. Lias, J.E. Bartmess, J.F. Liebmann, J.L. Holmes, R.D. Levin, W.C. Mallard, J. Phys. Chem. Ref. Data 17 (Suppl. 1) (1988).
[36] K. Kimura, S. Katsumata, Y. Achiba, T. Yamazaki, S. Iwata, Handbook of HeI Photoelectron Spectra of Fundamental Organic Molecules, Japan Scientific Society Press, Tokyo, 1981.
[37] S.G. Lias, H.M. Rosenstock, K. Deard, B.W. Steiner, J.T. Herron, J.H. Holmes, R.D. Levine, J.F. Liebman, S.A. Kafafi, J.E. Bartmess, E.F. Hunter, P.J. Linstrom, W.G. Malard, NIST Chemistry Webbook, 2004, http://webbook.nist.gov/chemistry.
[38] R. Wörgötter, J. Kubišta, J. Žabka, Z. Dolejšek, T.D. Märk, Z. Herman, Int. J. Mass Spectrom. Ion Processes 174 (1998) 53.
[39] O. Sekiguchi, V. Bakken, E. Uggerud, J. Am. Soc. Mass Spectrom. 15 (2004) 982.